

## MULTIPACTOR IN DIELECTRIC LOADED ACCELERATING STRUCTURES\*

P. Schoessow#, A. Kanareykin, C. Jing, Euclid Techlabs, 5900 Harper Rd, Solon, OH 44139  
 O. Sinitsyn, Institute for Research in Electronics and Applied Physics, University of Maryland,  
 College Park, MD 20742  
 W. Gai, J. Power, ANL, Argonne IL 60439

### Abstract

Significant progress has been made in the development of high gradient rf driven dielectric accelerating structures. As a consequence dielectric loaded accelerating structures are emerging as a possible, important future alternative to all metal based accelerating structures, facilitating the possibility of very high accelerating gradients and more compact and cost effective accelerators. One effect limiting further advances in this technology is the problem of multipactor.

The first high power experiments with an 11.424-GHz rf driven alumina accelerating structure exhibited single surface multipactor. Unlike the well understood multipactor problem for dielectric rf windows, where the rf electric field is tangential and the rf power flow is normal to the dielectric surface, strong normal and tangential rf electric fields are present from the  $TM_{01}$  accelerating mode in the DLA and the power flow is parallel to the surface at the dielectric-beam channel boundary. The fraction of the power absorbed at saturation in the DLA was found to increase with the incident power, with more than half of the incident power being absorbed. While a number of approaches have been developed, no one technology for MP mitigation is able to completely solve the problem.

In this paper we report on numerical calculations of the evolution of the MP discharge, and give particular attention to MP dependence on the rf power ramp profile, optimizing the device geometry, and the use of engineered surface features on the beam channel wall to interrupt the evolution of the multipactor discharge.

### INTRODUCTION

As various engineering challenges (breakdown, dielectric losses, efficient rf coupling) have been overcome, the technology of high gradient rf driven dielectric loaded structures appears increasingly attractive as a viable option for high energy accelerators. Multipactor has proven to be a factor in limiting the practicality of these devices. The accelerating mode in a DLA structure possesses a significant component of the electric field normal to the dielectric-beam channel boundary. The presence of both strong radial and axial electric fields leads to a new regime of single surface multipactor where only electrons emitted during a small fraction of the rf period contribute to multipactor. Saturation levels for multipactor in this regime are

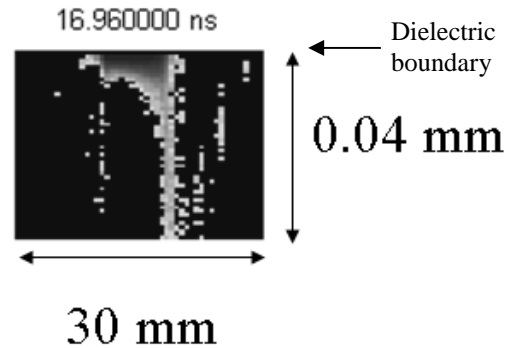


Figure 1: R-z plot of the secondary electron density near the dielectric-vacuum channel boundary in a developed MP discharge. The color scale is logarithmic.

significantly larger—corresponding to >50% power absorption—than the 1% power absorption by multipactor on an rf window.

For a multipactor discharge to be sustained, a number of conditions need to be simultaneously satisfied. The subset of emitted electrons that return to the dielectric-vacuum boundary and are resonantly captured must produce secondary electrons with a greater than unity yield; furthermore the secondaries must also be resonantly captured. As the discharge grows the electric field is modified by the contribution of the static space charge electric field, thus continuously changing the resonance condition.

The complexity of the single surface multipactor process makes its analytic treatment challenging. Nevertheless, an analytic model of the process has been developed by Power and Gold and is found to be in qualitative agreement with the experimental results [1]. Multipactor in this model is characterized by the ratio of the radial to axial electric fields at the dielectric-vacuum boundary  $E_r/E_z = \pi a/\lambda_z$ , where  $a$  is the radius of the beam channel and  $\lambda_z$  is the wavelength of the accelerating mode. The fraction of the incident power absorbed by the multipactor discharge is predicted by the model to scale as  $a^4$ .

In general reduction in the size of the beam channel seems to be advantageous from the standpoint of multipactor (although at the cost of making the transverse wakefields stronger and increasing the beam quality requirements). The ANL group was able to perform high power multipactor measurements on three X-band

\*Work supported by US DoE SBIR Program  
 #paul.schoessow@euclidtechlabs.com

structures made from alumina, MCT-20 ceramic, and fused silica.

Multipactor was observed in all three structures with the magnitude of the effect following the aperture size. The data was consistent with  $a^4$  scaling of the power absorption. Overall normalization differed by about 25% from that predicted; the discrepancy is attributed to the use of nominal SEE (secondary electron emission) parameters for the structure materials.

In the ANL/NRL measurements [2,3], the primary diagnostics were missing power (power absorbed by the multipactor discharge) and the intensity of light from the discharge measured using a CCD camera. The general technique is exemplified by the alumina structure measurement. Following initial rf conditioning, the incident ( $P_i$ ), reflected ( $P_r$ ), and transmitted ( $P_t$ ) rf power levels were measured with directional couplers as the incident power was varied from 5 kW to 5 MW in 150 ns

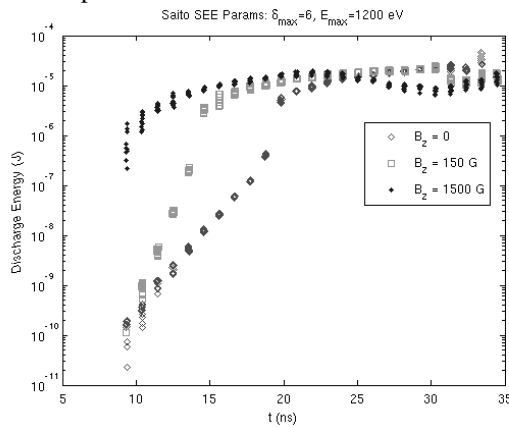


Figure 2: OOPIC-Pro simulation of time evolution of a MP discharge in the ANL alumina structure for a particular set of secondary emission parameters and different axial magnetic field strengths. The summed electron kinetic energy in the discharge is plotted vs time. Note the saturation intensities are nearly the same but the turn on profiles of the discharges differ significantly. Clusters of points in time correspond to sampling the numerical results over a complete rf period.

(FWHM) pulses, corresponding in turn to accelerating gradients of 25 kV/m to 8 MV/m. The measured power transmission and reflection coefficients ( $P_t/P_i$ ,  $P_r/P_i$ ) at low power were consistent with the bench test data. At high powers,  $P_i > 80\text{kW}$ ,  $P_t/P_i$  was found to decrease monotonically as a function of  $P_i$ , without a corresponding increase in the reflection coefficient. The increasing fraction of the incident power unaccounted for by transmission, reflection, or the attenuation expected in the structure is denoted the missing power and was observed to be about 50% of the incident power at the highest power used in the experiment. The measured missing power as a function of incident power has to date been the principal quantitative diagnostic in these DLA multipactor experiments. Light emission was also observed from the surface of the alumina, with an

intensity (measured by a CCD camera) proportional to the missing rf power.

To date we have used the OOPIC-Pro 2½D PIC code [10] as a primary modeling tool. These r-z geometry simulations are complementary to theory and modeling efforts at ANL and UMD which focus on r-φ analyses and permit us to study the axial development of the discharge. Use of a 2D code permits faster computations when performing the parameter sweeps that are necessary given the large parameter space for SEE characteristics.

## MULTIPACTOR MODELING

OOPIC-Pro is a 2½D FDTD electromagnetic PIC simulation code that incorporates the Vaughan model [11] for secondary electron emission.

Secondary emission boundary conditions are applied to the interior surface of the dielectric structure. Electrons striking this boundary produce multiple secondary electrons according to the Vaughan model described previously. In order to start the discharge a thin (one mesh cell) low current dc “seed” electron source is located on the interior wall at the halfway point in z. The turn on delay for the seed source can be specified relative to the rf phase.

OOPIC-Pro specifies a user-defined maximum number of macroparticles to be used in the simulation. In order to handle the exponential growth in the number of electrons during the discharge, the algorithm downsamples the number of particles by a factor of two when the number of macroparticles exceeds a predefined limit. The particle weights are scaled accordingly to conserve the total charge at the rescaling step. Typical total macroparticle populations used for these simulations were  $0.25 \times 10^6$ . (Since the electrons in the discharge tend to be concentrated in a thin layer near the interior surface of the structure, this number is adequate for these calculations.)

Because OOPIC-Pro is a time domain code it is necessary to generate the  $\text{TM}_{01}$  rf pulse using a sinusoidally varying current density  $j_z$  on axis at  $z = 0$ , and delay the onset of the multipactor discharge until the rf has filled the structure. Using the initial boundary dielectric section allows a pure  $\text{TM}_{01}$  mode to be generated without the fields in the neighborhood of the current source interacting with the electrons of the multipactor discharge. For parameter studies the rf fields at the point of onset of the discharge are saved to disk in hdf5 format during the initial run and read back for each successive run. In this way the initial rf fill calculation need only be performed once.

Because of the r-z geometry supported by OOPIC-Pro the MP discharge in this model is assumed to form as a uniform circular ring on the circumference of the dielectric vacuum channel. Thus the multipactor modeling based on this code treats only the axial evolution of the discharge. The light emitted from the discharges in the ANL experiment [3] was not strongly asymmetric in φ, so that use of a 2D simulation is not too inaccurate given the uncertainty in the SEE parameters.

By contrast, the Power-Gold analysis [1] does not include any longitudinal dependence of the discharge. The UMD group has developed an  $r$ - $\phi$  geometry multipactor simulation code [12] that extends the analysis of ref. [1] to a non-stationary model with self consistent handling of the space charge field. We will use this code to complement our existing calculation techniques. In particular, we plan to implement the capability of including axial grooves in the beam channel wall and study their effects on suppressing multipactor.

## SUPPRESSING MULTIPACTOR

One approach that has been suggested for avoiding multipactor in rectangular waveguides is to incorporate a grooved surface to act as a trap for secondary electrons [8,9] and thus interrupt the propagation of the discharge. Incorporating a similar mitigation scheme into cylindrical geometry dielectric structures is somewhat of a challenge. Axial channel grooves or vanes may serve a similar role in dielectric structures, with an axial applied magnetic field to curl up the secondaries. Simulation results (Fig.1) show that the discharge is localized very close to the vacuum channel boundary, suggesting that the characteristic size of the surface features required would have a minimal impact on the cavity fields.

However, the use of a dc field to suppress multipactor is not completely understood in that it seems to slightly enhance multipactor effects for smooth bore DLAs. This effect is observed experimentally as an increase in power absorption by the discharge. Simulations (Fig.2) show a magnetic field dependent rise time of the discharge although the asymptotic discharge intensities seem to be independent of the field.

Grooves or other surface features such as facets may also serve another function, that of spoiling the resonance conditions needed to sustain a multipactor discharge. We are investigating via simulations the effect of the modified geometry. We are investigating various channel geometries using numerical simulations to evaluate their efficacy in controlling multipactor. Diamond tooling could be used to inscribe the pattern of channels or facets on the interior of the dielectric device, since our ceramic structures cannot be manufactured with them in place.

Incorporating a similar mitigation scheme into cylindrical geometry dielectric structures is somewhat of a challenge. Axial channel grooves or vanes may serve a similar role in dielectric structures, with an axial applied magnetic field to curl up the secondaries. It is however necessary to point out that the use of a dc field to suppress multipactor is not completely understood in that it seems to slightly enhance multipactor effects for smooth bore DLAs. This effect is observed experimentally as an increase in power absorption by the discharge [4].

Grooves or other surface features such as facets may also serve another function, that of spoiling the resonance conditions needed to sustain a multipactor discharge.

Figure 3 shows an OOPIC model of the evolution of multipactor in the ANL alumina structure for 1W power

level and two sets of Vaughan parameters that have been reported for alumina surfaces. This suggests that a temporal diagnostic of the discharge (e.g. a streak camera analysis of the emitted light) with resolution  $\sim 100$  ps would be useful in constraining the characteristics of the multipactor discharge. It also gives some indication of the sensitivity of the discharge development to the secondary electron emission energy and yield.

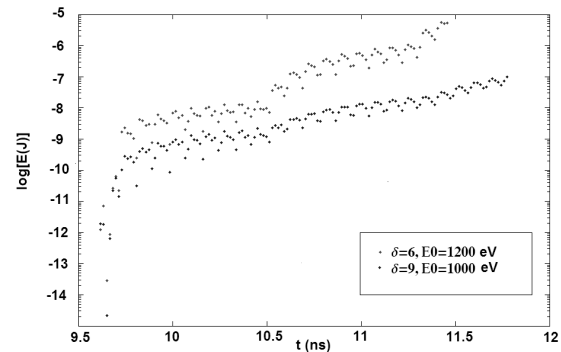


Figure 3: Early time simulation of MP discharge evolution for two sets of Vaughan parameters.

## SUMMARY

Multipactor discharge in an rf driven dielectric structure is a rich and complex area of study. Some of the areas that have been investigated include numerical simulations of the temporal and spatial evolution of the discharge as a function of the rf power and secondary emission characteristics of the dielectric and the effects of an external B field. We have begun examining mitigation possibilities including the incorporation of grooves, vanes, and channels to trap secondary electrons and spoil the multipactor resonance conditions. The use of  $r$ - $z$  geometry calculations complements other analytic and simulation efforts and allows the study of longitudinal effects in the evolution of the discharge.

## REFERENCES

- [1] J.G. Power, S. Gold, *Advanced Accelerator Concepts, 12<sup>th</sup> Workshop*, AIP CP877 (2006) p.362
- [2] Jing, C. *et al.*, *IEEE Trans. Plasma Sci.* **33** (2005) pp 1155-1160
- [3] J. G. Power *et al.*, *Phys. Rev. Lett.* **92**, 164801 (2004)
- [4] C. Jing *et al.*, *Proc. PAC 2005*, p.1566
- [5] W. Gai, A.D. Kanareykin, A.L. Kustov, J. Simpson, *Phys. Rev. E* **55**(3), pp. 3481-3488, (1997).
- [6] L.Wu, L.K.Ang, *Phys. Plasmas* **14** 013105 (2007)
- [7] C. Jing *et al.*, *Proc. PAC 2007*, p.3157
- [8] M.Pivi *et al.*, PAC05, paper ROPB001
- [9] M. Pivi *et al.*, PAC07, paper WEOAC01
- [10] [http://www.txcorp.com/products/OOPIC\\_Pro/](http://www.txcorp.com/products/OOPIC_Pro/)
- [11] J. Vaughan, *IEEE Trans. Electron Devices*, **36**(9) p.1963 (1989)
- [12] O.V.Sinitsyn *et al.*, *Proc. AAC08*, AIP CP1086